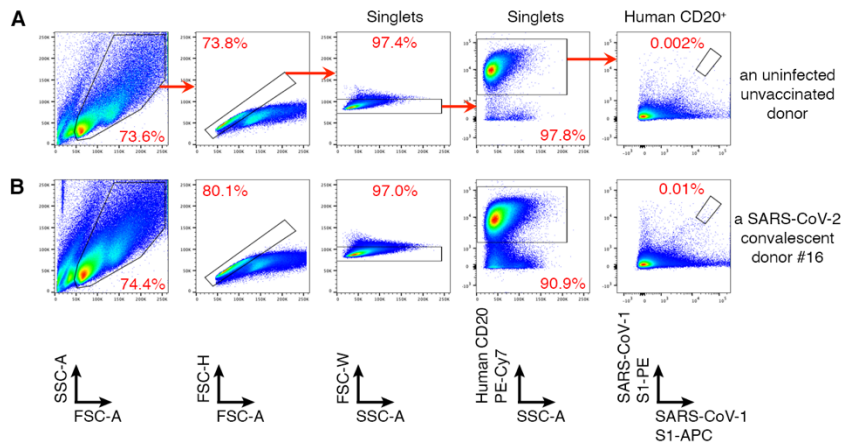


1 **SUPPLEMENTARY FIGURES AND LEGENDS**

2



3

4 **Figure S1. Gating strategy for B cell sorting.**

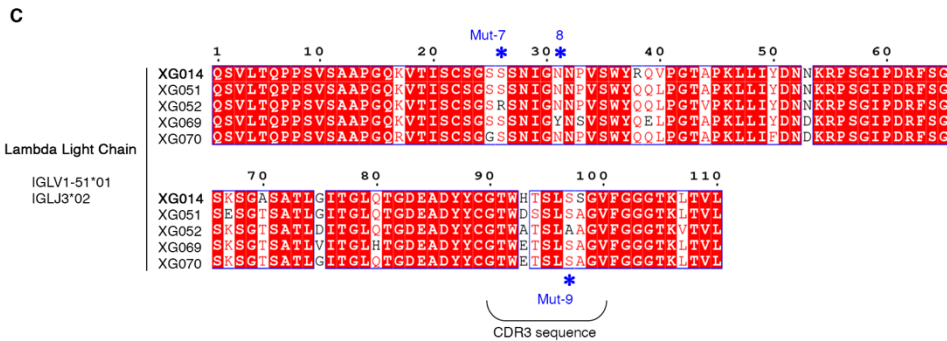
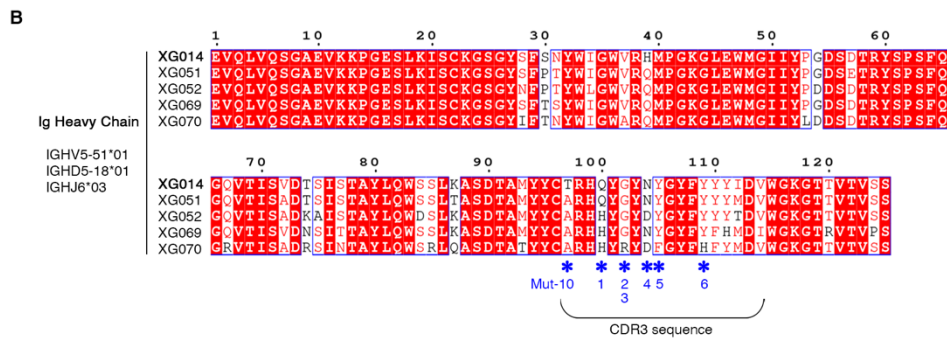
5 (A and B) Human memory B cells recognizing SARS-CoV-1 S1 protein were single-
6 cell sorted for antibody cloning. From left to right, each figure corresponds to the
7 sequential gating strategy. Frequencies of double positive (S1-PE⁺ S1-APC⁺) memory
8 B cells are shown in the right most panel. FSC, forward scatter; SSC, side scatter (-A,
9 area; -H, height; -W, width). Compared with the uninfected unvaccinated donor (A),
10 the percentage of memory B cells recognizing SARS-CoV-1 S1 antigen significantly
11 increased.

12

A

| | Ig heavy chain | | | | Ig light chain | | | |
|-------|----------------|------------------|----------|---------------------------|----------------|-------------|---------------|-------------|
| | V gene | D gene | J gene | CDR3 amino acid sequence | V gene | J gene | CDR3 sequence | |
| XG051 | IGHV5-51*01 | IGHD5-18*01 | IGHJ6*03 | ARHQYGYNYGYFYFYMDV | Lambda | IGLV1-51*01 | IGLJ3*02 | GTWDSLSAGV |
| XG052 | IGHV5-51*01 | IGHD5-18*01 | IGHJ6*03 | ARHHYGYDYGYFYFYTDV | Lambda | IGLV1-51*01 | IGLJ3*02 | GTWATSLAAGV |
| XG053 | IGHV4-59*01 | IGHD3-3*01 | IGHJ6*03 | AREGAERGDNNFWNGYTPLNYCMDV | Lambda | IGLV2-8*01 | IGLJ1*01 | SSYAVRNNFV |
| XG054 | IGHV4-39*01 | IGHD2-2*02 | IGHJ4*02 | ARNNVNLLRIPISLGFDS | Kappa | IGKV3-11*01 | IGKJ4*01 | QQYGNWPLT |
| XG055 | IGHV3-9*01 | IGHD3-10*01 | IGHJ4*02 | AKEGQVWVGEIWRSHFDY | Kappa | IGKV1-39*01 | IGKJ1*01 | QQSYLTPT |
| XG056 | IGHV3-30*04 | IGHD3-22*01 | IGHJ4*02 | ARGGKYDSSGFY | Lambda | IGLV2-11*01 | IGLJ2*01 | CSYAGSYTLGV |
| XG057 | IGHV3-11*01 | IGHD1-26*01 | IGHJ3*02 | ARAEWDPLRGGALDI | Kappa | IGKV3-15*01 | IGKJ2*01 | QQYDYWPGT |
| XG058 | IGHV2-70*11 | IGHD4-11*01 | IGHJ4*02 | ARMIVTSTYFDY | Lambda | IGLV2-8*01 | IGLJ2*01 | SSYAGSNNLV |
| XG059 | IGHV1-69*08 | IGHD2-8*01 | IGHJ3*02 | ARSLGPNGAVDI | Kappa | IGKV1-39*01 | IGKJ2*01 | QQSYTLPT |
| XG060 | IGHV1-18*01 | IGHD3-3*01 | IGHJ4*02 | ARDGRLAIFGWVIGGGYFDY | Lambda | IGLV2-14*01 | IGLJ3*02 | SSYTSSTTWW |
| XG061 | IGHV2-70*15 | IGHD5-12*01 | IGHJ4*02 | ARTRYGGYFELY | Kappa | IGKV4-1*01 | IGKJ4*01 | QQYYSTPLT |
| XG062 | IGHV3-13*01 | IGHD6-19*01 | IGHJ2*01 | ARVNYSSGWPLYWYCDL | Lambda | IGLV8-61*01 | IGLJ3*02 | VLYMDSGIWW |
| XG063 | IGHV3-30*04 | IGHD2-8*01 | IGHJ5*02 | ARASLPYCANGVCYCIDP | Lambda | IGLV1-44*01 | IGLJ3*02 | SAWDDSLNGWV |
| XG064 | IGHV3-74*01 | IGHD6-19*01 | IGHJ3*02 | TSLTGWSDVFDI | Lambda | IGLV8-61*01 | IGLJ2*01 | VLYMGSNDWV |
| XG065 | IGHV3-9*01 | IGHD4-17*01 | IGHJ4*02 | AKATTVTALIKSSFYD | Kappa | IGKV3-15*01 | IGKJ5*01 | QQYNNWPPGIT |
| XG066 | IGHV4-39*01 | IGHD2-2*01 | IGHJ4*02 | ARRGRYCSSTTCYEIDY | Lambda | IGLV2-8*01 | IGLJ2*01 | SSYAGSNIWI |
| XG067 | IGHV4-59*08 | IGHD5-18*01 | IGHJ6*03 | AGYSYGYVRYFYFMDV | Kappa | IGKV2-28*01 | IGKJ3*01 | MQALQTPFT |
| XG068 | IGHV4-59*01 | IGHD1-1*01 | IGHJ4*02 | ARYKDTTVLSPYFFDV | Kappa | IGKV4-1*01 | IGKJ2*01 | QQYATPYT |
| XG069 | IGHV5-51*01 | IGHD5-18*01 | IGHJ6*03 | ARHHYGYNYGYFYFHMDI | Lambda | IGLV1-51*01 | IGLJ3*02 | GTWETSLSAGV |
| XG070 | IGHV5-51*01 | IGHD4/OR15-4a*01 | IGHJ6*03 | ARHHYRYDFGYFHYFMDV | Lambda | IGLV1-51*01 | IGLJ3*02 | GTWETSLSAGV |
| XG014 | IGHV5-51*01 | IGHD5-18*01 | IGHJ6*03 | TRHQYGYNYGYFYFYIDV | Lambda | IGLV1-51*01 | IGLJ3*02 | GTWHTSLSSGV |

XG000 | RBD-binding XG000 | RBD-binding (weak) XG000 | NTD-binding XG000 | RBD- & NTD-binding XG000 | No antigen binding



13

14 **Figure S2. Sequence information of our cloned SARS-CoV-1-cross-reactive mAbs.**

15 (A) Detailed information of the 20 cloned mAbs. These mAbs have naturally paired

16 heavy and light chains. Variable (V), diversity (D) and joining (J) genes, and CDR3

17 amino acid sequences of both heavy and light chains are listed. Based on the ELISA

18 results, antibody names are color-coded: red, RBD-binding antibodies; orange, weak

19 RBD-binding antibodies; blue, NTD-binding antibodies; purple, antibodies binding

20 both RBD and NTD; and gray, no binding on the tested antigens. XG014 was isolated

21 previously from the same donor by using SARS-CoV-2 S-ECD as the bait protein ^{17,20}.

22 (B) Amino acid sequence alignment of five antibody family members, including XG051,

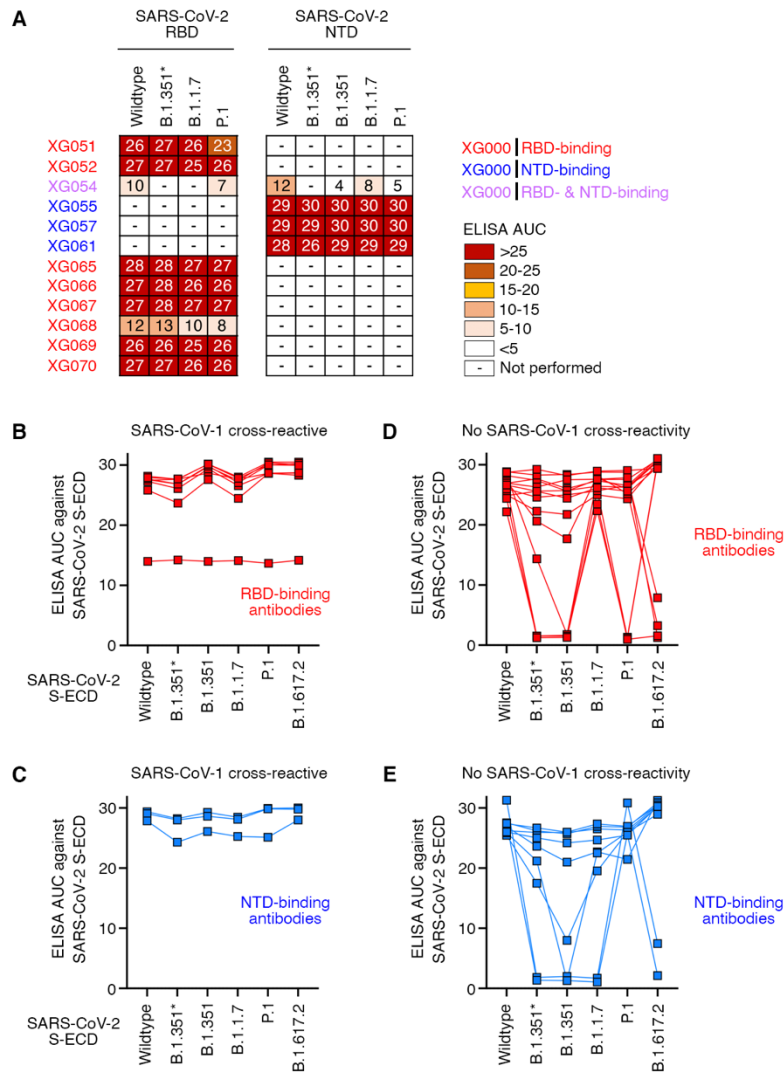
23 XG052, XG069, XG070, and XG014. These mAbs were originally from the same

24 expanded B cell clone, since they are encoded by the same Ig variable gene segments

25 with closely related CDR3 sequences. Ten amino acid residues for generating antibody

26 variants are marked by asterisks.

27



28

29 **Figure S3. ELISA assays for our cloned cross-reactive mAbs.**

30 (A) ELISA results against various recombinant RBD or NTD proteins. The area under
 31 the curve (AUC) values were calculated by PRISM.

32 (B) ELISA results for SARS-CoV-1-cross-reactive RBD-binding mAbs.

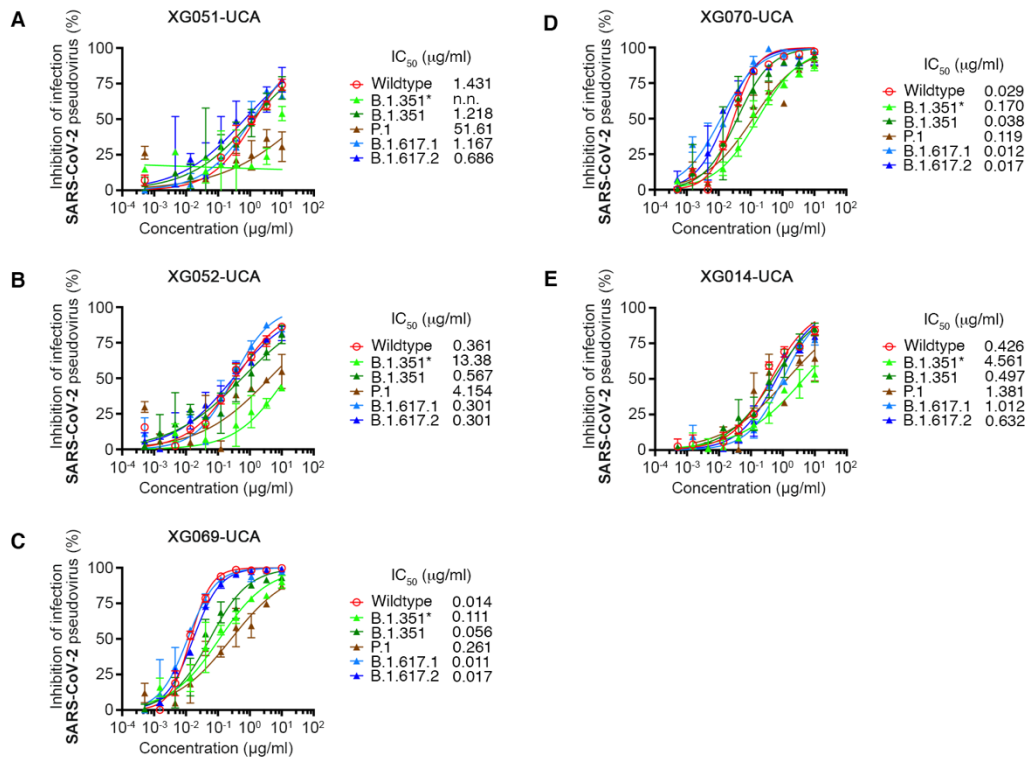
33 (C) ELISA results for SARS-CoV-1-cross-reactive NTD-binding mAbs.

34 (D) ELISA results for RBD-binding mAbs with no SARS-CoV-1 cross-reactivity.

35 (E) ELISA results for NTD-binding mAbs with no SARS-CoV-1 cross-reactivity. The

36 antigen proteins used in (B-E) were recombinant S-ECD proteins of wildtype SARS-

37 CoV-2 or its variants.

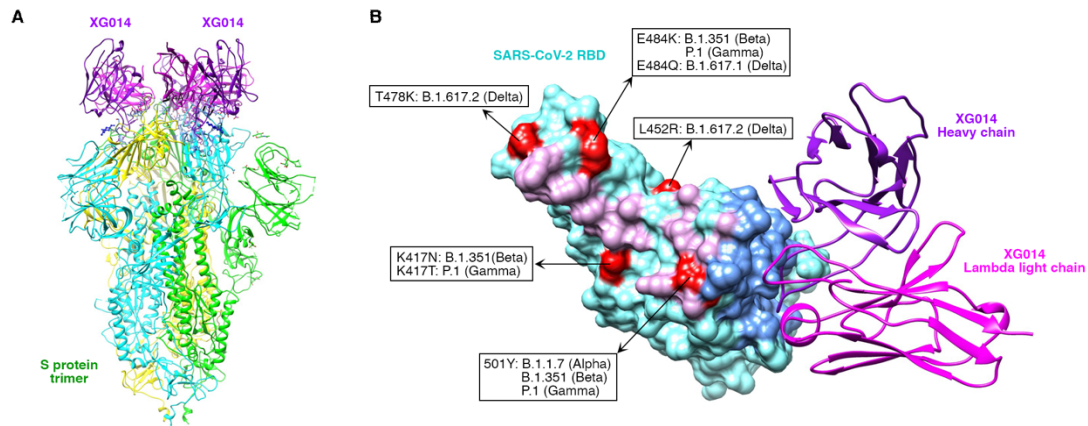


38

39 **Figure S4. In vitro neutralization assays of five unmutated common ancestor**
 40 **(UCA) antibodies.**

41 (A-E) XG051-UCA (A), XG052-UCA (B), XG069-UCA (C), XG070-UCA (D), and
 42 XG014-UCA (E) antibodies showed neutralizing activity against wildtype SARS-CoV-
 43 2 and several variants. Percent inhibition of infection was normalized to the luciferase
 44 signals in the control samples, which had no antibody added. The data are shown as
 45 mean ± SEM. The IC₅₀ values were calculated by nonlinear regression analysis in
 46 PRISM software.

47



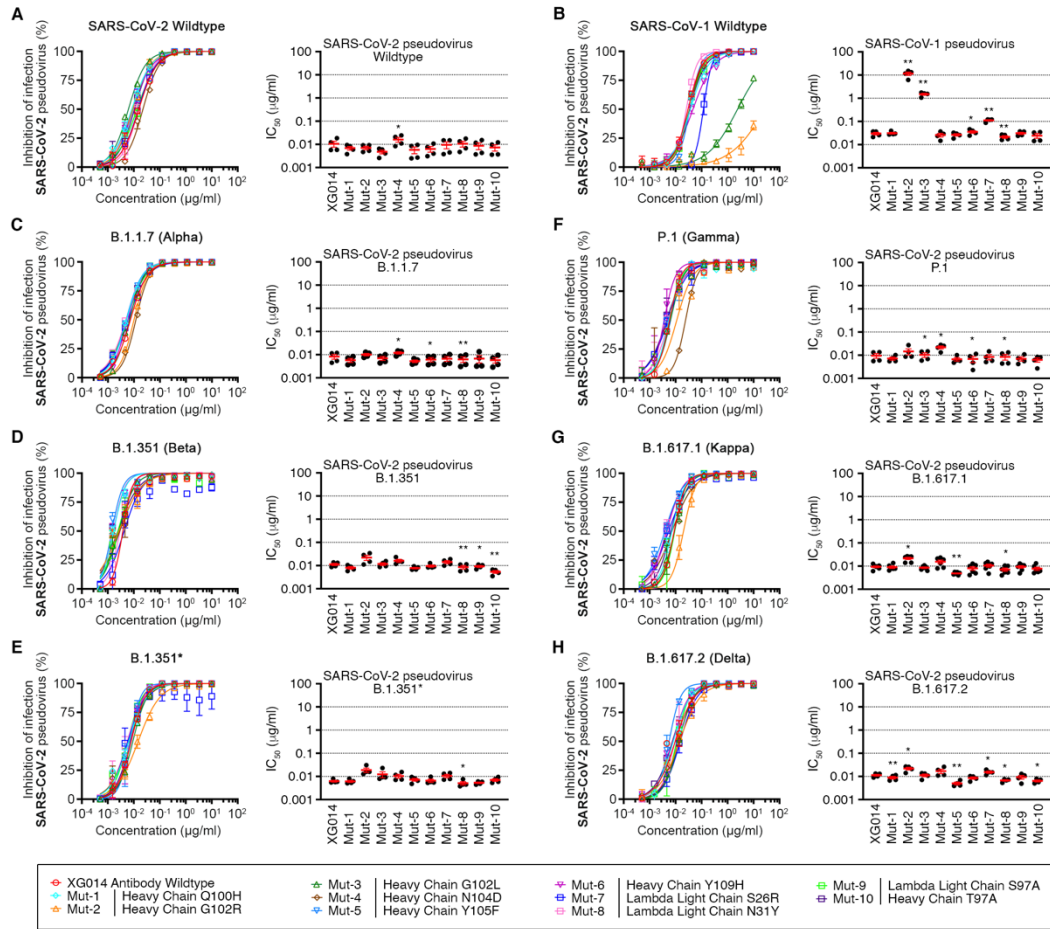
48

49 **Figure S5. Structural analysis of XG014-S trimer complex.**

50 (A) Cryo-EM structure of the XG014-S trimer complex (PDB ID 7V2A). XG014
 51 recognizes RBD epitope and locks three RBDs in “down” (closed) conformation²⁰. The
 52 immunoglobulin heavy/light chains of XG014 are colored in dark/light purple, while
 53 the three subunits of SARS-CoV-2 S trimer are colored as green, yellow, and cyan,
 54 respectively.

55 (B) Structural basis for the XG014 neutralization breadth against SARS-CoV-2 VOCs,
 56 except Omicron. The molecular surface of SARS CoV-2 RBD (cyan), together with
 57 XG014 heavy/light chains (dark/light purple), showed that the popular escape mutation
 58 sites (red) are located outside of the interaction surface of XG014-RBD (blue).

59

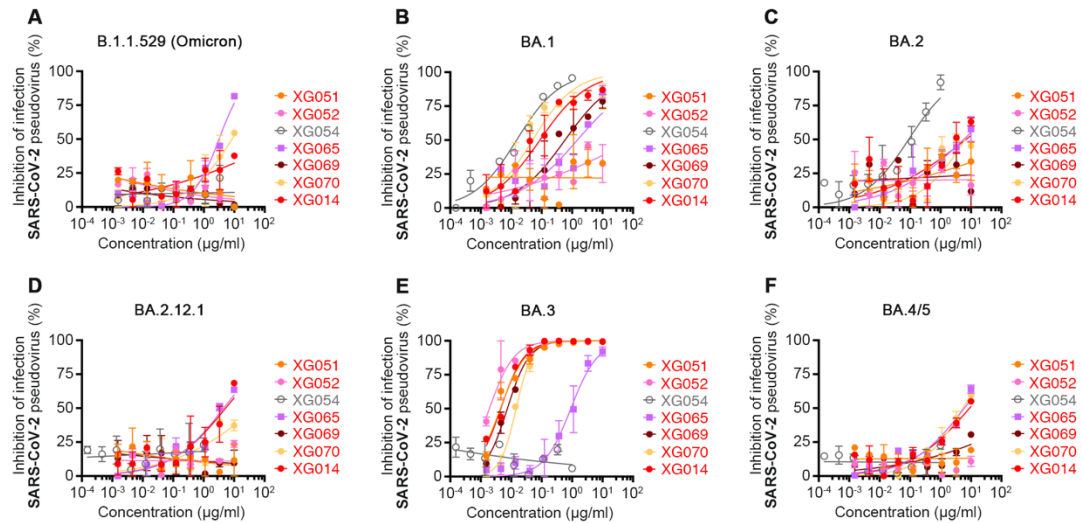


60

61 **Figure S6. In vitro neutralization assays to identify the key amino acid residues**
 62 **for XG014 neutralization potency and breadth.**

63 (A-H) Neutralizing activities of XG014 and its 10 antibody variants, Mut-1~10, against
 64 wildtype SARS-CoV-2 (A), wildtype SARS-CoV-1 (B), B.1.1.7 (Alpha) (C), B.1.351
 65 (Beta) (D), B.1.351* (E), P.1 (Gamma) (F), B.1.617.1 (Kappa) (G), and B.1.617.2
 66 (Delta) (H). The data are shown as mean ± SEM. The IC₅₀ values were calculated by
 67 nonlinear regression analysis in PRISM software. Statistical analysis was performed
 68 using the Wilcoxon rank-sum test, and the p values are indicated by stars, * p < 0.05;
 69 ** p < 0.01.

70

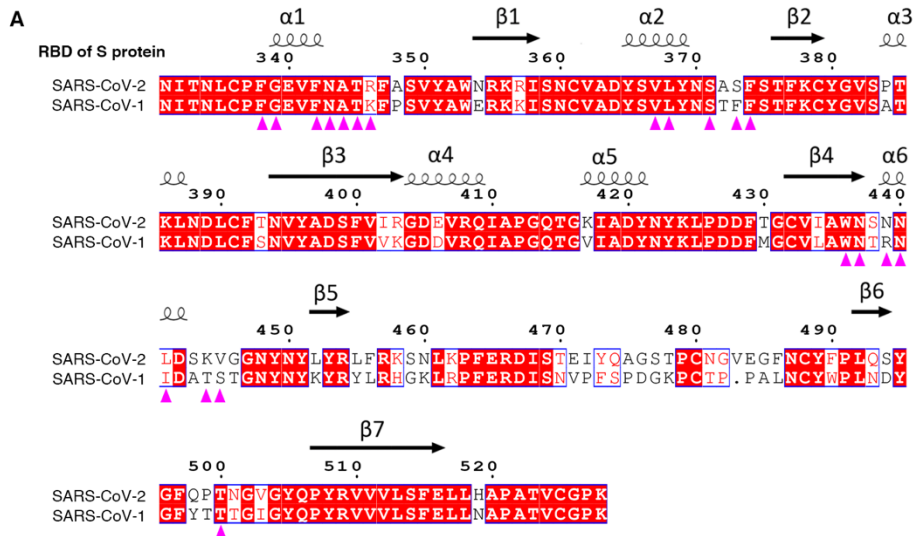


71

72 **Figure S7. In vitro neutralization assays against pseudoviruses of Omicron**
 73 **sublineages using the seven SARS-CoV-1-cross-reactive mAbs.**

74 (A-F) The neutralizing activities of the seven cloned cross-reactive mAbs, XG051,
 75 XG052, XG054, XG065, XG069, XG070, and XG014, varied considerably against
 76 SARS-CoV-2 Omicron sublineages. Percent inhibition of infection was normalized to
 77 the luciferase signals in the control samples, which had no antibody added. The data
 78 are shown as mean \pm SEM.

79



B

| B.1.1.529 | BA.1 | BA.2 | BA.2.12.1 | BA.3 | BA.4/5 |
|--|--|----------------------------------|----------------------------------|----------------------------------|----------------------------------|
| | | T19I L24S del25/27 | T19I L24S del25/27 | | T19I L24S del25/27 |
| A67V del69/70 T95I | A67V del69/70 T95I | | | | del69/70 |
| G142D | G142D | G142D | G142D | | G142D |
| del143/145 del211 L212I | del143/145 N211I del212/212 | | | | |
| ins214EPE | | V213G | V213G | | V213G |
| G339D S371L S373P S375F | G339D S371L S373P S375F | G339D S371F S373P S375F | G339D S371F S373P S375F | | G339D S371F S373P S375F |
| | | T376A D405N R408S | T376A D405N R408S | | T376A D405N R408S |
| K417N N440K G446S | | K417N N440K | K417N N440K | | K417N N440K |
| | | | L452Q | | L452R |
| S477N T478K E484A | S477N T478K E484A | S477N T478K E484A | S477N T478K E484A | | S477N T478K E484A F486V |
| Q493R G496S Q498R N501Y Y505H T547K | Q493R G496S Q498R N501Y Y505H T547K | Q493R Q498R N501Y Y505H | Q493R Q498R N501Y Y505H | | Q498R N501Y Y505H |
| D614G H655Y N679K P681H | D614G H655Y N679K P681H | D614G H655Y N679K P681H | D614G H655Y N679K P681H | D614G H655Y N679K P681H | D614G H655Y N679K P681H |
| N764K D796Y N856K Q954H N969K L981F | N764K D796Y N856K Q954H N969K L981F | N764K D796Y | N764K D796Y | N764K D796Y | N764K D796Y |

Receptor-binding domain (RBD)

80

81 **Figure S8. Comparison of S protein sequences.**

82 (A) Amino acid sequence alignment of RBD regions from SARS-CoV-1 and SARS-
83 CoV-2. The highly conserved amino acid residues between these two different viruses
84 are marked in red. The amino acid residues involved in XG014-RBD interaction are

85 indicated by purple triangles.

86 (B) Amino acid mutations in the S protein of B.1.1.529 (Omicron) and its sublineages,

87 BA.1, BA.2, BA.2.12.1, BA.3, BA.4, and BA.5, compared with wildtype SARS-CoV-

88 2. The amino acid sequences of BA.4 and BA.5 S proteins are exactly the same.

89

| | Wildtype | B.1.1.7 (Alpha) | B.1.351 (Beta) | P.1 (Gamma) | B.1.617.2 (Delta) | B.1.1.529 (Omicron) | SARS-CoV-1 |
|---------|----------|--------------------|-------------------|----------------|----------------------|------------------------|------------|
| K398.22 | 31 | 20 | 9 | 11 | 8 | 6 | 32 |
| 47D11 | 78 | 40 | 38 | 40 | 17 | 1392 | 40 |
| BG10-19 | 8 | 3 | 5 | 4 | 1 | >5000 | 75 |
| H014 | 389 | 214 | 173 | 85 | 75 | 83 | 583 |

| IC ₅₀ (ng/ml) |
|--------------------------|
| 0-50 |
| 50-100 |
| 100-500 |
| 500-1000 |
| 1000-5000 |
| >5000 |

90

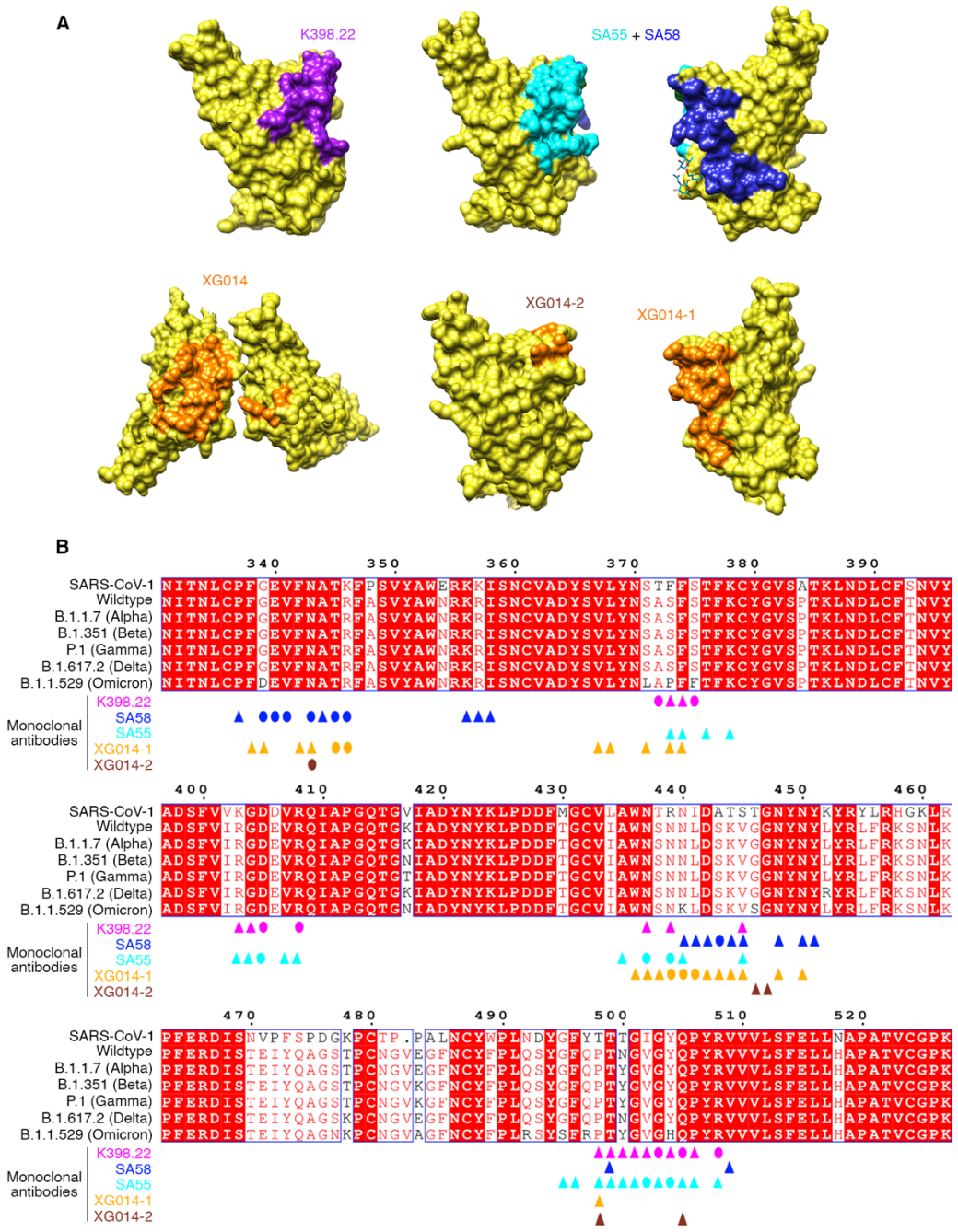
91 **Figure S9. IC₅₀ values for several mAbs cross-neutralizing SARS-CoV-1.**

92 Calculated IC₅₀ values based on our in vitro neutralization assays. Four reported anti-

93 SARS-CoV-2 bNAbs with cross-neutralizing activity against SARS-CoV-1 include

94 K398.22³⁴, 47D11³⁰, BG10-19³¹, and H014⁵³.

95



96

97 **Figure S10. Comparison of K398.22, SA58, SA55, and XG014 epitopes.**

98 (A) RBD model shown in surface mode with the epitope of K398.22 shown in purple

99 (PDB ID 7TP4).

100 (B) RBD surface with SA58 and SA55 epitopes shown in cyan and blue, respectively

101 (PDB ID 7Y0W).

102 (C) RBD surface with XG014 epitopes shown in orange (PDB ID 7V2A).

103 (D) Sequence alignment of RBDs from SARS-CoV-1, SARS-CoV-2 wildtype and five
104 SARS-CoV-2 VOCs. Conserved amino acids are highlighted as red. Residues involved
105 in K398.22, SA58, SA55, and XG014 interactions are marked with triangles in purple,
106 cyan, blue, and orange, respectively. Residues involved in strong interactions (hydrogen
107 bonds and salt bridges) are marked with circles.